Contribution from the Department of Chemistry,
Texas A&M University, College Station, Texas 77843

New Multidentate Ligands. XV. Chelating Tendencies of Diglycine-*N,N*-diacetic Acid, Triglycine-*N,N*-diacetic Acid, and Tetraglycine-*N,N*-diacetic Acid[1]

R. J. MOTEKAITIS and A. E. MARTELL*

Received September 4, 1973

The synthesis and quantitative equilibrium studies of three new oligopeptide derivatives, diglycine-*N,N*-diacetic acid (2GDA), triglycine-*N,N*-diacetic acid (3GDA), and tetraglycine-*N,N*-diacetic acid (4GDA), are described in detail. Their metal ion–proton–ligand reaction stoichiometries have been determined, and the corresponding equilibrium constants were calculated from the potentiometric data. The probable structures of the chelate species in aqueous solution as a function of pH were deduced from a detailed analysis of the carbonyl region of infrared spectra measured in D_2O and from a comparison of the available data with analogous peptides and other reference compounds. At low pH, the initial binding of Cu(II), Ni(II), Co(II), Zn(II), and Fe(III) takes place at the diacetic acid end of the molecule. As the pH is raised Co(II) and Cu(II) each assist the displacement of one amido proton from 2GDA and two protons from 3GDA and 4GDA. Ni(II) displaces only one amide proton from 3GDA and two amido protons from 4GDA, but none from 2GDA. Assignments of some new, unusually low amide carbonyl stretching frequencies were made possible in this study.

Introduction

Recently, it has been shown that suitably designated multidentate ligands are useful in demonstrating new properties of individual ligand donor groups.[2,3] Thus, the synthetic ligands DGENTA (diglycylethylenediaminetetraacetic acid) and EDDAG-DA (*N,N'*-ethylenediaminediacetylglycine-*N,N'*-diacetic acid) provided the interesting and previously unknown examples of metal ion promoted dissociation of amide protons in aqueous solution by Co(II) and Fe(III) ions.[2] Since then, the binding characteristics of the hydroxamide groups[3] with selected metal ions have been determined using the technique of incorporating the specific group being studied into a multidentate ligand to keep the metal:ligand ratio fixed. These auxiliary groups serve the function of keeping the metal ions in solution until the pH can be raised sufficiently for the group under study to react with the metal ion.

This continuing study of metal ion interaction in aqueous solution with important, nonconventional coordinating groups such as amides, hydroxamide, hydrazide, imide, peptide, hydroxyalkyl, hydroxyaryl, etc., has already yielded much useful new information. This paper describes the chemistry of three new multidentate ligands containing the peptide group, which is contained in the *N,N*-diacetic acid derivatives of diglycine (2GDA), triglycine (3GDA), and tetraglycine (4GDA).[4] Previous investigations[5-7] of the parent peptides suffered from complications caused by the formation of complexes containing two and three ligand anions per metal ion, along with the 1:1 complex under study. In this investigation, however, 1:1 reaction stoichiometry was ensured by the derivatization of the oligopeptides.

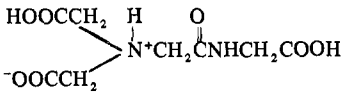

2GDA

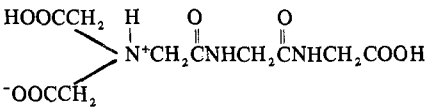

3GDA

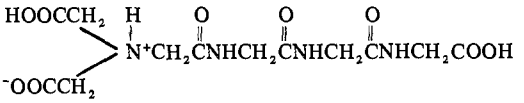

4GDA

Experimental Section

Reagents. 2GDA, 3GDA, and 4GDA. In a general procedure, either diglycine (20 mmol), triglycine (10 mmol), or tetraglycine (4.0 mmol) was mixed with twice the number of millimoles of bromoacetic acid in 25 ml of water. Sodium hydroxide solution (10 *M*) was added dropwise at 30–35°. After 3 hr, the reaction mixture was passed through Dowex 50W-X8 resin (H^+ form) and was eluted with water. The strong acid fraction was discarded and the eluate was concentrated. After a short time the product crystallized.

Anal. Calcd for $C_8H_{12}N_2O_7$ (2GDA): C, 38.7; H, 4.9; N, 11.2. Found: C, 38.7; H, 5.0; N, 10.8. Calcd for $C_{10}H_{15}N_3O_8$ (3GDA): C, 39.4; H, 5.0; N, 13.8. Found: C, 39.4; H, 4.8; N, 13.5. Calcd for $C_{12}H_{18}N_4O_9$ (4GDA): C, 39.7; H, 5.0; N, 15.5. Found: C, 39.0; H, 4.9; N, 16.1.

Bromoacetic acid (Aldrich) and oligopeptides (Nutritional Biochemicals) were used as received. Reagent grade metal nitrate salt solutions were standardized chelatometrically with EDTA. NaOD solution was purchased from Bio-Rad.

Measurements. A sample of 0.10–0.15 mmol of solid ligand (molecular weight determined by titration) together with a 1:1 ratio (also 1:2 in the case of 2GDA) of metal to ligand was diluted to 40.0[c] or 50.00 ml with water in a sealed, thermostated (25.00 ± 0.05°) potentiometric equilibrium vessel equipped with Beckman E-2 glass and calomel electrodes, an N_2 inlet and bubbler outlet, and a graduated microburet. The test solution, adjusted to 0.100 *M* in KNO_3, was titrated with 0.10 *M* standard CO_2-free KOH while $-\log [H^+]$ was measured on a Beckman Research pH meter calibrated with strong acid and strong base so as to read directly in hydrogen ion concentration [$pK_w = -\log ([H^+][OH^-])$ was 13.792]. The maximum excursion between calculated and observed values of pH in this calibration was ±0.006 pH unit throughout the pH range of 2–11. In this paper the term pH is used synonymously with $-\log [H^+]$.

The infrared spectra were measured using a Beckman IR-12 spectrophotometer with 0.10 *M* D_2O solutions in 0.050-mm matched AgCl cells.

(1) This work was supported by a research grant, No. A-259, from the Robert A. Welch Foundation.

(2) (a) R. J. Motekaitis and A. E. Martell, *J. Amer. Chem. Soc.*, 92, 4223 (1970); (b) R. J. Motekaitis and A. E. Martell, paper presented at the 158th National Meeting of the American Chemical Society, New York, N. Y., Sept 1969.

(3) R. J. Motekaitis, I. Murase, and A. E. Martell, *J. Coord. Chem.*, 1, 77 (1971).

(4) A preliminary report of this work was presented by R. J. Motekaitis and A. E. Martell, 27th Southwest Regional Meeting of the American Chemical Society, San Antonio, Tex., Dec 1971.

(5) A. E. Martell in "Recent Topics in Coordination Chemistry," S. Misume and K. Ueno, Ed., Special Publication No. 84, Nankado, Tokyo, Japan, 1968, pp 47–67.

(6) M. Kim and A. E. Martell, *J. Amer. Chem. Soc.*, 89, 5138 (1967).

(7) A. Kaneda and A. E. Martell, to be submitted for publication.

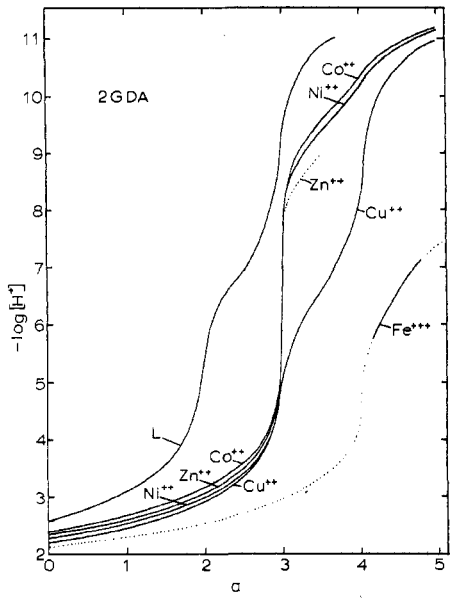

Figure 1. Potentiometric equilibrium curves for the 1:1 molar ratios of metal ions to 2GDA. Dotted lines indicate precipitation; a is the number of moles of 0.10 M potassium hydroxide added per mole of ligand; concentrations are 0.0025 M in ligand and metal salts; solution contains 0.100 M KNO_3; $T = 25°$.

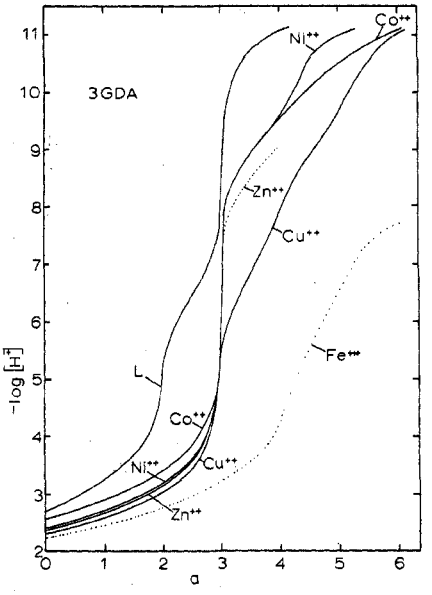

Figure 2. Potentiometric equilibrium curves for the 1:1 molar ratios of metal ions to 3GDA. Dotted lines indicate precipitation; a is the number of moles of 0.10 M potassium hydroxide added per mole of ligand; concentrations are 0.0025 M in ligand and metal salts; solution contains 0.100 M KNO_3; $T = 25°$.

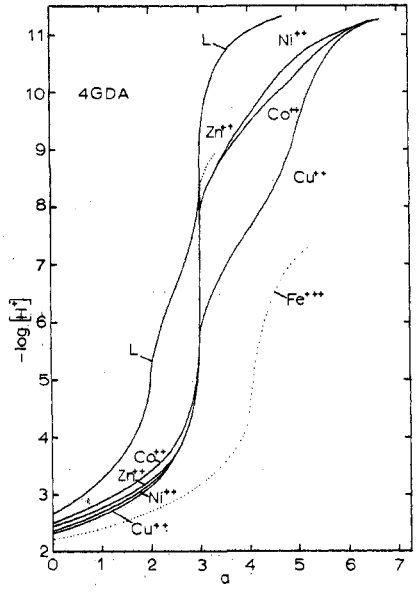

Figure 3. Potentiometric equilibrium curves for the 1:1 molar ratios of metal ions to 4GDA. Dotted lines indicate precipitation; a is the number of moles of 0.10 M potassium hydroxide added per mole of ligand; concentrations are 0.0025 M in ligand and metal salts; solution contains 0.100 M KNO_3; $T = 25°$.

Results

Ligands. The potentiometric titration curves of 2GDA, 3GDA, and 4GDA (=H_3L) are shown as the top trace in Figures 1-3. In each case, two protons per ligand molecule dissociate between $a = 0$ and $a = 2$ (where a is the moles of NaOH added per mole of ligand present) and at higher pH an additional proton dissociates in a buffer region between $a = 2$ and $a = 3$. The protonation constants describing these ligand curves and calculated[8] by a program developed in these laboratories are listed in Table I.

Low-pH *N*GDA Complexes. The 1:1 *N*GDA curves with Ni(II), Cu(II), Co(II), Zn(II), and Fe(III) are shown in Figures 1-3. There is a striking similarity in the buffer regions between $a = 0$ and $a = 3$ for all the metals tested, and it was determined that the equilibria up to $a = 3$ could be described in terms of ligand protonation and metal complexation equilibria as represented in eq 1 and 2. The Fe(III) curve in each

$$M^{n+} + L^{3-} \rightleftharpoons ML^{(n-3)+} \qquad K_{ML} \qquad (1)$$

$$ML^{(n-3)+} + H^+ \rightleftharpoons MHL^{(n-2)+} \qquad K^H_{ML} \qquad (2)$$

case yielded a precipitate at about $a = 0$.

The equilibrium constants describing the formation leg of each equilibrium curve to $a = 3$ were calculated using an iterative procedure of varying K^H_{ML} to find the best values of K_{ML} at each titration point. The best values of K_{ML} and K^H_{ML} were considered to be that choice of K^H_{ML} which minimized the average deviation of K_{ML} calculated at each experimental point in the interval $a = 0$ and $a = 3$ of the potentiometric equilibrium curve. A more detailed account of the calculation procedure has been described recently.[2a] The values of these constants together with the average deviations listed in parentheses are listed in Table II.

High-pH Metal Ion–*N*GDA Interaction. The 1:1 systems of 2GDA (Figure 1) with Co(II), Ni(II), and Cu(II) each exhibit a one-proton buffer region after $a = 3$, while Zn(II) precipitates immediately after this inflection. Iron(III) is unique, because its 2GDA chelate is soluble only between a values of 4 and 5.

Beyond $a = 3$ the 3GDA curves (Figure 2) with metal ions differ from the 2GDA ligand curves in that both Co(II) and Cu(II) possess two-proton buffer regions and in that the Fe(III) complex does not redissolve at any pH. Ni(II) shows only one proton dissociated between 3 and 4 equiv of base,

Table I. Protonation Constants[a] of *N*GDA in Aqueous Solution

	a	log K^H_1	log K^H_2	log K^H_3
2GDA	0.016	6.92	3.31	2.11
3GDA	0.009	6.56	3.55	2.14
4GDA	0.007	6.34	3.45	2.22

[a] $K^H_n = [H_nL^{(n-3)+}]/[H^+][H_{n-1}L^{(n-4)+}]$.

(8) R. J. Motekaitis, I. Murase, and A. E. Martell, *J. Inorg. Nucl. Chem.*, 33, 3353 (1971).

Table II. Logarithms of Stability Constants[a]

Ligand[b]	Equilibrium constants[c]	Metal ions				
		Cu^{2+}	Ni^{2+}	Co^{2+}	Zn^{2+}	Fe^{3+}
2GDA	K_{ML}	~11.4 (1)	8.69 (2)	7.44 (1)	7.94 (1)	10.56 (1)
	K^{H}_{ML}	3.14 (1)	3.00 (1)	3.03 (1)	3.01 (1)	~1.6 (2)
	K_{A_1}	6.61 (4)		9.35 (1)		6.62 (3)
3GDA	K_{ML}	~11.0 (4)	8.02 (1)	6.84 (2)	7.63 (1)	10.01 (1)
	K^{H}_{ML}	3.42 (1)	3.39 (1)	3.33 (1)	3.21 (1)	2.00 (1)
	K_{A_2}	8.93 (2)	8.97 (5)	10.10 (1)		
	K_{A_1}	6.91 (2)		9.01 (1)		
4GDA	K_{ML}	8.79 (1)	7.62 (1)	6.45 (2)	7.00 (1)	9.99 (1)
	K^{H}_{ML}	3.58 (1)	3.46 (1)	3.47 (1)	3.41 (1)	1.87 (2)
	K_{A_2}	8.21 (2)	10.24 (2)	9.79 (2)		
	K_{A_1}	7.05 (2)	9.02 (2)	9.14 (2)		

[a] $T = 25°$, $\mu = 0.100$ (KNO_3). [b] 2GDA = diglycine-*N,N*-diacetic acid, 3GDA = triglycine-*N,N*-diacetic acid, 4GDA = tetraglycine-*N,N*-diacetic acid. [c] Equilibrium constants defined by eq 1-5.

while Zn(II) precipitates immediately after the inflection at $a = 3$.

The 4GDA titration data (Figure 3) reveal that for Ni(II), Co(II), and Cu(II), two (and only two) additional protons are neutralized after the $a = 3$ inflection point, whereas Zn(II) and Fe(III) behave in their usual fashion.

The complex equilibria at higher pH values (after $a = 3$) are therefore represented by eq 3-5. The values of the amide

$$MH_{-1}L^{(n-4)+} + H^+ \rightleftharpoons ML^{(n-3)+} \qquad K_{A_1} \qquad (3)$$

$$MH_{-2}L^{(n-5)+} + H^+ \rightleftharpoons MH_{-1}{}^{(n-4)+} \qquad K_{A_2} \qquad (4)$$

$$MH_{-3}L^{(n-6)+} + H^+ \rightleftharpoons MH_{-2}{}^{(n-5)+} \qquad K_{A_3} \qquad (5)$$

proton association constants were calculated by a refinement procedure[8] which calculates back the titration curve from the stability constants. This calculation is identical with the one used in the calculation of protonation constants. The results of these calculations are listed in Table II.

Infrared evidence confirmed that the reaction taking place in the high-pH buffer region of (2GDA)Ni^{II} corresponds to eq 6, since no amidic protons dissociate upon addition of

$$NiLOH^{2-} + H^+ \rightleftharpoons NiL^- \qquad K_x \qquad (6)$$

base beyond $a = 3$. The calculated value for log K_x is 9.50.

Infrared Spectra. The ir spectra of diglycine-*N,N*-diacetic acid and of its Cu(II) chelates in aqueous solution are presented in Figures 4 and 5. Similar spectra were also obtained for 2GDA with Co(II), Ni(II), and Zn(II) and for 3GDA and 4GDA with and without these divalent metal ions. The ir spectra were studied in detail as a function of added base using an approach similar to that employed in the polypeptide work.[9] Detailed assignments of the specific bands for all species in solution were then made starting from the dipeptide derivatives and working toward the tetrapeptide compound. Frequencies of the ir absorption bands and their assignments are presented in Tables III-V. Justification of these assignments, an explanation of the relationship of the assigned spectra to the conclusions based on potentiometric data, and conclusions concerning the structures of the species in solution are given in the Discussion.

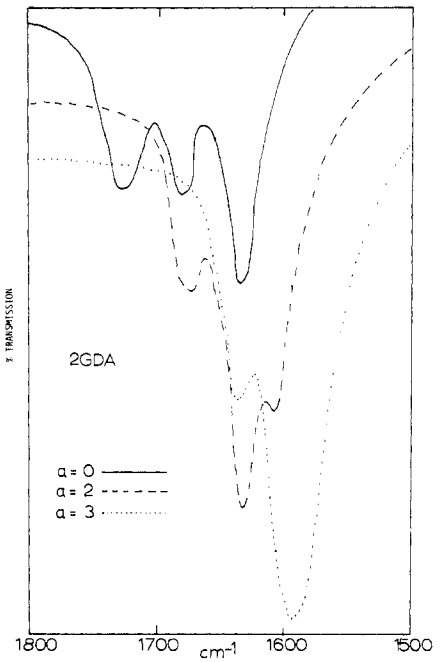

Figure 4. Infrared spectra of diglycine-*N,N*-diacetic acid in D_2O solutions as a function of base added; a is the number of moles of NaOD added per mole of ligand present; concentration of 2DGA is 0.1 *M* measured in 0.05-mm matched AgCl cells.

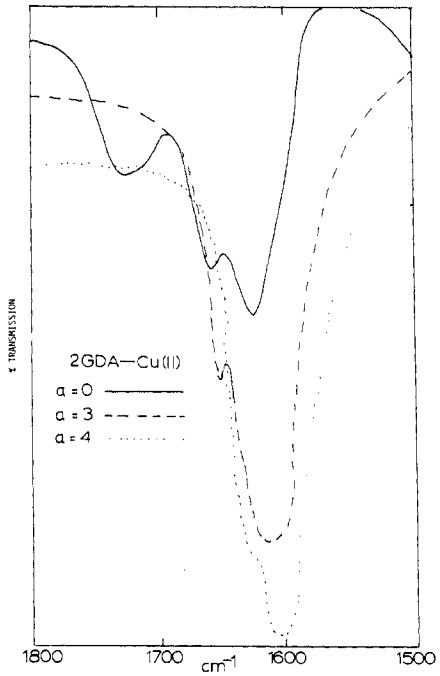

Figure 5. Infrared spectra of 2GDA-Cu(II) complexes in D_2O solutions as a function of base added; a is the number of moles of NaOD added per mole of ligand present; concentration of 2GDA and Cu(II) is 0.1 *M* measured in 0.05-mm matched AgCl cells.

Discussion

Potentiometric Studies. *N*GDA. The values of the protonation constants listed in Table I for the three ligands (*N*GDA = 2GDA, 3GDA, 4GDA) are consistent with the structures of these ligands. In Table VI a comparison is made of group basicities with those of reference compounds containing similar groups. The peptide group present in 2GDA exerts a considerable electron-withdrawing inductive effect on the basic terminal amino group lowering its pK_a (log K^{H}_1) by $10^{2.41}$, when compared with iminodiacetic acid (IDA).[10] The nitrogen pK_a for *N*-(carbamoylmethyl)iminodiacetic

(9) A. E. Martell and M. Kim, submitted for publication in *Inorg. Chem.*

(10) L. C. Thompson, *Inorg. Chem.*, **1**, 490 (1962). $pK_a(N)$ = 9.33 in IDA.

Table III. Infrared Spectra of 2GDA (cm^{-1})

Species	$-COOH$	$-{}^{+}CONH-$	$-{}^{2+}CONH-$	$-CONH-$	$-\overset{\overset{O\cdots M^{2+}}{\|}}{C}NH-$	$-\overset{\overset{M^{2+}}{\|}}{C}ON^{-}-$	$-{}^{+}COO^{-}$	$-COO^{-}\cdots M^{2+}$	$-COO^{-}$	$-{}^{-}COO^{-}\cdots M^{2+}$	$-{}^{-}COO^{-}$
$H_3L^{\pm}$	1730	1680					1635				
HL^{2-}		1675					1632		1607		
L^{3-}				1635					1588		
CuHL	1725		1660					1627			
CuL^{-}			1655					∿1625	∿1610		
$CuH_{-1}L^{2-}$						∿1612 sh		∿1625 sh			1600
NiHL	1730				1644			1616			
NiL^{-}					1646			1615	1603		
CoHL	1727				1645			1625			
CoL^{-}					1647			1615	1603		
$CoH_{-1}L^{2-}$						1580		∿1620		1594	

Table IV. Infrared Spectra of 3GDA (cm^{-1})

Species	$-COOH$	$-{}^{+}CONH-$	$-{}^{2+}CONH-$	$-CONH-$	$-\overset{\overset{O\cdots M^{2+}}{\|}}{C}NH-$	$-\overset{\overset{M^{2+}}{\|}}{C}ON^{-}-$	$-{}^{+}COO^{-}$	$-COO^{-}\cdots M^{2+}$	$-COO^{-}$	$-\overset{\overset{M^{2+}}{\|}}{C}ON^{-}-$
$H_3L^{\pm}$	1730	1682		1660 sh			1635			
HL^{2-}		1680		∿1660 sh			1631		1600	
L^{3-}				1642					1588	
CuHL	1725		∿1675 sh	1655				1626		
CuL^{-}			∿1670 sh	1650				∿1620	1605	
$CuH_{-1}L^{2-}$				∿1650 sh		Buried		1623	1695	
$CuH_{-2}L^{3-}$						Buried		1623	1593	1565
NiHL	1730			∿1660 sh	1647			1618		
NiL^{-}				∿1660 sh	1645			1615	1600	
$NiH_{-1}L^{2-}$					∿1650 sh	Buried		1618	1594	
CoHL	1728			∿1665 sh	1643			∿1620 sh		
CoL^{-}				∿1660 sh	1644			∿1613 sh	1600	
$CoH_{-1}L^{2-}$					∿1645 sh	∿1595		∿1620 sh	∿1595	
$CoH_{-2}L^{3-}$						∿1590		1618		∿1570
						∿1598 sh				

Table V. Infrared Spectra of 4GDA (cm^{-1})

Species	–COOH	–$^{+}$CONH–	–$^{2+}$CONH–	–CONH–	O···M^{2+} –CNH–	–CON–M^{2+}	–$^{+}$COO^{-}	–COO^{-}···M^{2+}	–COO^{-}	–CON–M^{2+} –CON–
$H_3L^{\pm}$	1730	∿1680 sh		∿1665 sh			1640			
				1650						
HL^{2-}		∿1680 sh		∿1665 sh			1640		1592	
				∿1652 sh						
L^{3-}				1648					1590	
CuHL	1726		∿1680 sh	∿1668 sh				∿1630		
				1655						
CuL^{-}			∿1675 sh	∿1668 sh				1619	1605	
				1650						
$CuH_{-1}L^{2-}$				∿1653 sh	∿1635 sh	∿1608		1624	1601	1563
$CuH_{-2}L^{3-}$					1626				1598	
									∿1612	
NiHL	1729			∿1670 sh	1649			1620	1601	
NiL^{-}				∿1670 sh	1647			1615		
$NiH_{-1}L^{2-}$				∿1652	1642	Buried		1618	1596	1557
$NiH_{-2}L^{3-}$					1645			1628	1592	
CoHL	1729			∿1660 sh	1647			1621		
CoL^{-}				1670	1648			1613	1602	
				1663						
$CoH_{-1}L^{2-}$				∿1670	1645	1599		1615		
$CoH_{-2}L^{3-}$					1645			∿1613	1596	1570

Table VI. Comparative Basicities (Protonation Constants) of Ligands

log K^{H}_{n}, this research	log K^{H}_{n}, model compounds
	Terminal Nitrogen
6.92 (2GDA)	8.14 (diglycine)[a]
6.56 (3GDA)	7.94 (triglycine)[a]
6.34 (4GDA)	7.90 (tetraglycine)[a]
	9.33 (iminodiacetic acid)[b]
	Peptide Carboxylate
3.31 (2GDA)	3.15 (diglycine)[a]
3.55 (3GDA)	3.26 (triglycine)[a]
3.45 (4GDA)	3.27 (tetraglycine)[a]
	Acetic Acid Carboxylate
2.11 (2GDA)	2.58 (iminodiacetic acid)[b]
2.14 (3GDA)	2.30 (carbamoylmethyliminodiacetic acid)[c]
2.22 (4GDA)	

[a] Reference 7. [b] L. C. Thompson, *Inorg. Chem.*, 1, 490 (1962). [c] G. Schwarzenbach, G. Anderegg, and H. Senn, *Helv. Chim. Acta*, 38, 1147 (1955).

acid (CMIDA) is 6.60,[11] a value which is very close to that of 2GDA. As the peptide chain length is increased (3GDA and 4GDA), a further drop in the basicity of this amino group is indicated. This drop arises from the cumulative long-range inductive effects of the several peptide groups present.

The peptide (C-terminal) carboxylate protonation constant (log K^{H}_{2}) in *N*GDA is just a few tenths of a log unit larger than the corresponding constant of the parent peptide. This, taking into account the relative distances of separation between functional groups, enables one unequivocally to assign the protonation scheme of the *N*GDA ligands as shown in the equation

$$\begin{aligned}
&{}^{-}OOCCH_2 \\
&\qquad\diagdown \\
&\qquad\quad N(CH_2CONH)_xCH_2COO^{-} \overset{H^+}{\rightleftharpoons} \\
&\qquad\diagup \\
&{}^{-}OOCCH_2 \\
&\qquad\quad L^{3-} \\
&{}^{-}OOCCH_2 \\
&\qquad\diagdown \\
&\qquad\quad NH^{+}(CH_2CONH)_xCH_2COO^{-} \overset{H^+}{\rightleftharpoons} \\
&\qquad\diagup \\
&{}^{-}OOCCH_2 \\
&\qquad\quad HL^{2-} \\
&{}^{-}OOCCH_2 \\
&\qquad\diagdown \\
&\qquad\quad NH^{+}(CH_2CONH)_xCH_2COOH \overset{H^+}{\rightleftharpoons} \\
&\qquad\diagup \\
&{}^{-}OOCCH_2 \\
&\qquad\quad H_2L^{-} \\
&HOOCCH_2 \\
&\qquad\diagdown \\
&\qquad\quad NH^{+}(CH_2CONH)_xCH_2COOH \qquad (7) \\
&\qquad\diagup \\
&{}^{-}OOCCH_2 \\
&\qquad\quad H_3L
\end{aligned}$$

Low-pH Chelates of *N*GDA. The similarity of the titration curves shown in Figures 1-3 for the divalent ions at low pH indicates that Cu(II), Ni(II), Co(II), and Zn(II) behave similarly in 1:1 metal ion–*N*GDA systems. In each case the initial complex formed up to the potential break at $a = 3$ is most reasonably concluded to be a substituted IDA type chelate. The formation constants (log K_{ML}) for Cu(II)-, Ni(II)-, Co(II)-, and Zn(II)-IDA complexes are 10.63, 8.19, 6.97, and 7.27.[12] In the present study, Table II, the formation constants for the corresponding reactions to form 1:1 chelates are of comparable magnitude, with a trend that is very similar to that found for the metal-IDA chelates.

(11) G. Schwarzenbach, G. Anderegg, and H. Senn, *Helv. Chim. Acta*, 38, 1147 (1955).
(12) G. Anderegg, *Helv. Chim. Acta*, 47, 1801 (1964).

Furthermore, the values of the chelate protonation constants vary in a manner which reveals the structures of the chelates formed in solution. Thus the values of log K^{H}_{ML} are larger for Cu(II) than for the other metals, whose values are rather similar but slightly lower. Also, in going from 2GDA to 3GDA, there is a larger step in K^{H}_{ML} than in going from 3GDA to 4GDA. The values of log K^{H}_{ML} approach log K^{H}_{2} as the molecule becomes longer. The distances between coordinated and uncoordinated donor groups, as implied from a reasonable interpretation of the above-mentioned trends in K^{H}_{ML}, coupled with the established fact that in ligands possessing the IDA-CH_2CONHR grouping, the initial complex formed is the IDA type with the neighboring amido carbonyl participating in hexacoordinate metal complexes and nonparticipating in the tetracoordinate planar copper(II) complex, uniquely predict structures I and II for the lower pH chelates.

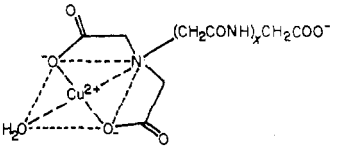

I, Cu(II)-*N*GDA chelate, CuL^-
x = number of peptide bonds

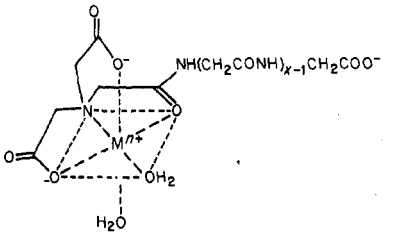

II, Ni(II)-, Co(II)-, Zn(II)-, and Fe(III)-*N*GDA chelates, $ML^{(n-3)+}$

Although Fe(III) is interesting in its own right, it cannot be dealt with quantitatively owing to the presence of a precipitate throughout the titration curves, except $a = 4$ to $a = 5$ for Fe-2GDA. Although unproven, a likely explanation for this phenomenon is that the soluble chelate is $FeH_{-1}L(OH)^{2-}$.

Metal Chelates of *N*GDA at High pH. When Figures 1-3 are examined more closely, it can be safely concluded that Cu(II) and Co(II) each displace an amidic proton from 2GDA (Ni(II) is ruled out on the basis of ir evidence), Cu(II) and Co(II) displace two and Ni(II) displaces only one peptide proton from 3GDA, and Cu(II), Ni(II), and Co(II) displace only two amidic protons each from 4GDA.

It is informative to compare the metal-assisted peptide proton-releasing abilities of the *N*GDA complexes to those of the parent polyglycines. Table VII shows that peptide proton displacement in the oligopeptide derivatives (*N*GDA) is lowered by one or two orders of magnitude, as the result of competing acetate groups.

In one previous case[2a] where auxiliary acetate substituents were present in a ligand containing amido groups, log K_{A1} was found to be 6.89 for Cu(II). This value is extremely close to those of the corresponding *N*GDA complexes of copper(II).

Infrared Spectra of Ligands. The infrared spectra of *N*GDA ligands measured as a function of equivalents of base added confirm the protonation scheme (eq 7) postulated on the basis of comparison of acidity constants and on previous experience.

2GDA. At low pH, $a = 0$, where the form of the ligand is primarily the neutral form, H_3L, the carbonyl infrared region consists of three peaks. The 1730-cm^{-1} absorption belongs to the protonated carboxylate, the 1680-cm^{-1} band to the amido group, and the remaining 1635 cm^{-1} to the carboxylate group. This assignment is consistent with the published spectrum of IDA,[13] whose un-ionized carboxylate absorption is at 1721 cm^{-1}, while the absorption of the ionized carboxylate is found at 1619 cm^{-1}. It also agrees with the spectrum of monoprotonated diglycine[9] which shows the un-ionized carboxylate at 1720 cm^{-1} and the amido group close to a positively charged amino nitrogen atom at 1675 cm^{-1}. It is also significant that the ionized carboxylate absorption is considerably more intense than either the neutral amido group or the un-ionized carboxylate absorption.

Table VII. Amide Protonation Constants in *N*GDA Chelates and in Reference Systems

	log K_{A1}		log K_{A2}		log K_{A3}	
	Cu^{2+}	Ni^{2+}	Cu^{2+}	Ni^{2+}	Cu^{2+}	Ni^{2+}
2G	4.58					
2GDA	6.61					
3G	5.20	8.74	6.71	7.84		
3GDA	6.91	8.97	8.93			
4G	5.40	∿8.0	6.79	∿8.0	9.09	∿8.0
4GDA	7.05	9.02	8.21	10.24		
EDDAG-DA	6.89[a]					

[a] Reference 2a.

As base is added, at $a = 2$, the species is predominantly HL^{2-} (eq 7). The amide absorption remains essentially unchanged at 1675 cm^{-1} which is interpreted as indicating that the amino nitrogen still remains protonated. Also, the ionized acetic acid carboxylate absorption remains fixed in position at 1632 cm^{-1} yet grows considerably signifying the further deprotonation of this carboxylate group. However, the terminal carboxylate upon deprotonation shifts all the way down to 1607 cm^{-1}. This compares well with diglycine in the HL form, for which the carboxylate absorption was measured by Martell and Kim[9] at 1607 cm^{-1}.

Further deprotonation ($a = 3$) causes the amide to absorb now at 1635 cm^{-1} and the absorption of the acetic acid carboxylates to join the low-frequency peaks of the terminal carboxylate (1600 cm^{-1}) at 1588 cm^{-1}. Both of these shifts of approximately 40 cm^{-1} are indicative of the deprotonation of the terminal amino nitrogen.

3GDA. This ligand possesses one more amido group than 2GDA, which is further removed from the direct electrostatic influence of the protonated amino nitrogen and therefore absorbs closer (at 1660 cm^{-1}) to the normal amide stretching frequency[14] of polypeptides, at about 1650 cm^{-1}. Otherwise, the other absorptions are very similar to those shown for 2GDA. The HL^{2-} species predominates at $a = 2$ and its spectrum is also very similar to that of 2GDA at $a = 2$, with the exception of the shoulder at *ca.* 1660 cm^{-1} which is the absorption of the second amido group. The terminal carboxylate is now at 1600 cm^{-1} (*vs.* 1607 cm^{-1} for 2GDA) perhaps reflecting the overall influence of the electron-withdrawing amide groups on the carboxylate frequency. Final deprotonation of 3GDA at $a = 3$ shows an amide absorption of both amide groups at 1642 cm^{-1} and the absorptions of the ionized acetic acid carboxylates at 1588 cm^{-1} with an apparent shoulder at *ca.* 1605 cm^{-1} for the ionized terminal carboxylate.

4GDA. When three amido groups are present, in 4GDA, at

(13) K. Nakamoto, Y. Morimoto, and A. E. Martell, *J. Amer. Chem. Soc.*, 84, 2081 (1962).
(14) L. J. Bellamy, "The Infrared Spectra of Complex Molecules," Wiley, New York, N. Y., 1962, p 228.

$a = 0$ the one closest to the positive nitrogen absorbs at about *ca.* 1680 cm^{-1} and the middle one at about 1665 cm^{-1}, while the group closest to the terminal carboxylate apparently does not feel the positive charge at all and absorbs at 1650 cm^{-1}. The protonated and ionized carboxylate absorptions are normal at 1730 and at 1637 cm^{-1}, respectively.

At $a = 2$, the nitrogen bears a formal charge of 1+ (as at $a = 0$) and therefore the three peptide carbonyl absorptions remain essentially fixed at 1680, 1665, and 1652 cm^{-1}. The acetic acid carboxylate absorptions also remain fixed at 1640 cm^{-1} and the terminal ionized carboxylate absorbs even lower at 1592 cm^{-1}.

The spectrum of the totally deprotonated 4GDA ($a = 3$) shows only two absorptions with no readily discernible shoulders. The peak at 1648 cm^{-1} represents the amide stretching frequencies, slightly raised over those of L^{3-} of 3GDA, which reflects the additional amide $-I$ effect; and the peak at 1590 cm^{-1} contains the three negative carboxylate absorptions.

Cu(II)-*N*GDA. From a comparison of K^{H}_{ML} with K^{H}_{2} (both COOH terminal dissociations) it was already concluded from potentiometric data that Cu^{2+}-*N*GDA complexes of the MLH and ML^- type are simply of the substituted IDA type with very little interaction of the coordinated metal ion with the adjacent amide carbonyl through coordination with it. An examination of the infrared spectra confirms this result to be the case.

Cu(II)-2GDA. At $a = 0$, the complex CuHL is about 90% formed so that the spectrum suffers very little ligand interference. The terminal un-ionized carboxylate absorbs at 1725 cm^{-1}, the amido carbonyl absorbs at 1660 cm^{-1}, and the coordinated carboxylates (to Cu^{2+}) show a strong band at 1627 cm^{-1}. It can be argued that the amido carbonyl is essentially uncoordinated because of the small shift of this band in going from 1675 cm^{-1} for HL^{2-} to 1660 cm^{-1} for MHL, where the monopositive proton on the amino nitrogen was replaced by a dipositive metal ion whose effect is in general more diffuse than that of a proton. If the amide carbonyl were coordinated through the oxygen, then the expected absorption would occur at even a lower frequency.

With the removal of a proton from the terminal carboxylate ($a = 3$) a spectrum of ML^- is obtained with the band at 1725 cm^{-1} disappearing and appearing at 1610 cm^{-1} as the absorption of a terminal uncoordinated carboxylate. The amido group absorbs unchanged at 1655 cm^{-1} and the coordinated carboxylates are also essentially unchanged in position at *ca.* 1625 cm^{-1}. Thus the structure of CuL^- may be safely represented by I.

$CuH_{-1}L^{2-}$ ($a = 4$) possesses a dissociated amide coordinated to the Cu^{2+} ion. That the structure of this species is represented by III can be inferred from the spectrum which shows

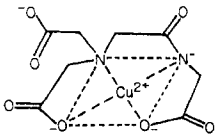

$CuH_{-1}L^{2-}$, 2GDA
III

an absorption band at *ca.* 1612 cm^{-1} for the dissociated and N-coordinated peptide link, a band at *ca.* 1625 cm^{-1}, and one at 1600 cm^{-1}. These latter two bands are due to the coordinated acetate carbonyl stretching mode without and with an adjacent ionized amido group. Since its absorbance is hidden, it is difficult to draw conclusions about the nature of the idle carboxylate of the acetic acid.

Cu(II)-3GDA. The IDA-type complex of 3GDA with copper(II) exhibits a spectrum similar to that of the 2GDA-Cu^{2+} system. At $a = 0$, the terminal protonated carboxylate absorbs at 1725 cm^{-1} and the coordinated diacetic acid carboxylates show a peak at 1626 cm^{-1}. The two amide groups are at *ca.* 1675 and 1655 cm^{-1}. Removal of the terminal carboxylate proton at $a = 3$ shifts the 1725-cm^{-1} absorption down to 1605 cm^{-1}. The coordinated IDA carboxylates (*ca.* 1620) and the two amido group absorptions (*ca.* 1670 and 1650 cm^{-1}) remain vitually unchanged in position. When further base is added, the peptide protons are removed in succession. At $a = 4$, only one amido group is visible as a shoulder at *ca.* 1650 cm^{-1} (O-coordinated amido) whereas the nitrogen-coordinated one is buried beneath the absorptions at 1623 cm^{-1} (coordinated acetic acid) and 1595 cm^{-1} (ionized uncoordinated terminal carboxylate and uncoordinated acetic acid). The structure of this complex is IV. At $a = 5$ (see V) both of the coordinated ionized amido group

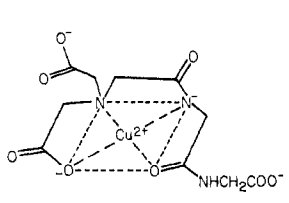

$CuH_{-1}L^{2-}$, 3GDA
IV

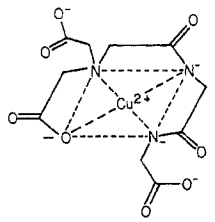

$CuH_{-2}L^{3-}$, 3GDA
V

absorptions are buried beneath the 1623-cm^{-1} (coordinated acetic acid) band and the 1593-cm^{-1} (ionized, uncoordinated acetic acid carboxylate and C-terminal carboxylate) band. There is however an absorption at 1565 cm^{-1} which is assigned to the adjacent negative N-coordinated amido groups. This latter assignment will become unquestionably certain when the case of Cu(II)-4GDA will be considered below.

Cu(II)-4GDA. At $a = 0$ the predominant species is CuHL where the copper ion resides coordinated on the diacetic acid end, with little interaction upon the neighboring amido group. The frequency of this amido group is *ca.* 5 cm^{-1} higher than the corresponding absorption in the 3GDA-Cu^{2+} system owing to the additional amide present. The other two amides absorb at *ca.* 1668 and 1655 cm^{-1}, in favorable agreement with the bare ligand. The protonated carboxylate (1726 cm^{-1}) and the coordinated diacetic acid carboxylates (*ca.* 1630 cm^{-1}) are in their usual positions.

At $a = 3$, the predominant species is CuL^- (I), and the main change in the spectrum is the disappearance of the 1726-cm^{-1} band and the appearance of the 1605-cm^{-1} band assigned to the deprotonated uncoordinated terminal carboxylate. The slight decrease in the position of the coordinated IDA carboxylates may be related to the acquisition of one unit of charge by the chelate. The amido carbonyl absorbs in a similar position as the protonated chelate does.

With further deprotonation at $a = 4$ (VI), $CuH_{-1}L^{2-}$ species forms with the two unionized amides absorbing at *ca.* 1653 and at 1635 cm^{-1} as a shoulder on the 1624-cm^{-1} band assigned to one coordinated IDA carboxylate. The ionized, coordinated amide absorption is buried somewhere at *ca.* 1608 cm^{-1} next to the ionized terminal carboxylate and acetate at 1601 cm^{-1}.

It was deduced from potentiometry that at $a = 5$ the formula for the sole species in solution must be $CuH_{-2}L^{3-}$. The sharp and strong peak at 1563 cm^{-1} for this species cannot be assigned to any other vibrations than the two adjacent, ionized, N-coordinated amide carbonyl stretching modes. As

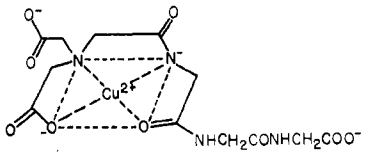

$CuH_{-1}L^{2-}$, 4GDA
VI

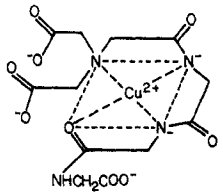

$CuH_{-2}L^{3-}$, 4GDA
VII

confirmation for structure VII of this complex, the third O-coordinated amide absorbs at 1626 cm^{-1}, some 10 wave numbers lower from the case at $a = 4$. This small shift indicates the effect of the adjacent negative charge. The remaining free carboxylates absorb at 1598 (C-terminal) and 1612 cm^{-1} (diacetate). Another arrangement consistent with the infrared spectra and the potentiometric results is not possible for $CuH_{-2}L^{3-}$.

Ni(II)-*N*GDA. It is anticipated (and will be borne out in the subsequent discussion) that the low-pH chelates of the substituted IDA type of Ni^{2+} with *N*GDA contain considerable interaction of the metal ion with the neighboring (to the amino group) amide carbonyl oxygen. This is true in the IDA-moiety-containing ligands such as DGENTA[2a] and as shall be seen in the present case.

Ni(II)-2GDA. The neutral chelate NiHL even at $a = 0$ shows considerable ionization of the terminal carboxylate group by the presence of an ir absorption at 1603 cm^{-1}. In addition, this chelate absorbs at 1644 cm^{-1}, which is the amide carbonyl. Therefore, from the fact that the terminal carboxylate is more acidic and from the fact that the amido group frequency was decreased relative to the Cu case, it is clear that the carbonyl in question is formally coordinated to the Ni^{2+} ion. The undissociated carboxylate absorption is at 1730 cm^{-1}, and the IDA portion, coordinated to the metal ion, absorbs at 1616 cm^{-1}, slightly lower than the copper analog.

At $a = 3$, NiL^- is the only species, and its absorbance differs essentially only in that the protonated carboxylate peak has disappeared in favor of a taller peak at the ionized carboxylate position at 1603 cm^{-1}. Thus II would best represent NiL^- as well as NiHL (with a proton on the C-terminal carboxylate).

At $a = 4$, a blue solution formed, which shortly thereafter precipitated as $Ni(OH)_2$.

Ni(II)-3GDA. At $a = 0$, there is a conspicuous absence of an ionized carboxylate at *ca.* 1600 cm^{-1}, indicative of the insulating effect of the extra amino acid moiety in 3GDA and expressed in terms of a higher K^{H}_{ML} over that of 2GDA. The extra peptide group absorbs at *ca.* 1660 cm^{-1} with the O-coordinated amide at 1647 cm^{-1}, similar to the previous case. Upon deprotonation of this chelate, at $a = 3$, the carboxylate is found to absorb at 1600 cm^{-1}, slightly lower due to the cumulative effect of the two amide groups present. The IDA-coordinated carboxylates are at 1615 cm^{-1}.

With $a = 4$ (VIII), one amide proton is lost. The undissociated O-coordinated amide absorbs at *ca.* 1650 cm^{-1}; the dissociated amide probably absorbs at about 1600 cm^{-1}, with its exact position being obscured by the 1618-cm^{-1} peak (coordinated acetic acid carboxylates) and by the ionized uncoordinated carboxylate at 1594 cm^{-1}. As indicated potentiometrically, further proton displacement by Ni(II) was found to be impossible.

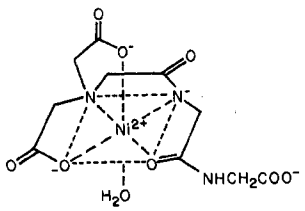

$NiH_{-1}L^{2-}$, 3GDA
VIII

Ni(II)-4GDA. The NiHL neutral species absorbs at 1729 (neutral terminal carboxylate), 1620 (coordinated diacetic acid carboxylates), 1649 (coordinated amide adjacent to coordinated amine), and *ca.* 1670 (sh) cm^{-1} (free amides in tetrapeptide). Similarly, NiL^- at $a = 3$ absorbs at 1601 (free ionized terminal carboxylate), 1615 (coordinated diacetates), 1647 (O-coordinated amido group), and *ca.* 1670 cm^{-1} (uncoordinated amido groups).

When further base is added to $a = 4$ (IX), one peptide proton dissociates, with a concomitant change in the spectrum. Although, the nitrogen-coordinated peptide is buried somewhere between the 1618-cm^{-1} (coordinated diacetic acid carboxylates) and the 1596-cm^{-1} (uncoordinated terminal ionized carboxylate) bands, the oxygen-coordinated middle amide vibration is discernible at 1642 cm^{-1} and the uncoordinated terminal amide as a shoulder at *ca.* 1652 cm^{-1}.

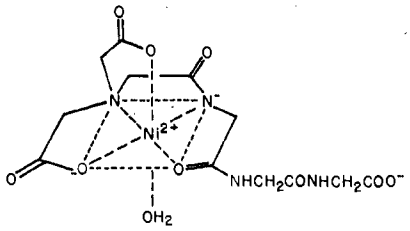

$NiH_{-1}L^{2-}$, 4GDA
IX

Five equivalents of base added produces the ultimate second dissociation of an amide group with their absorptions at 1557 cm^{-1}. This absorption is about 8 cm^{-1} lower than the "analogous" Cu^{2+} complex case, possibly showing the effect of further buildup of negative charge around the six-coordinate metal. The oxygen-coordinated third amide group absorbs at 1645 cm^{-1}. The coordinated diacetic acid group frequency is raised somewhat to 1628 cm^{-1}, and the uncoordinated terminal ionized carboxylate is lowered to 1592 cm^{-1} by virtue of the overall trinegative charge on the chelate. Structure X is proposed as the species in solution for $NiH_{-2}L^{3-}$.

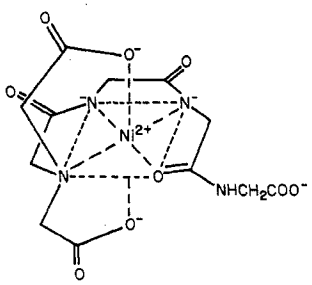

$NiH_{-2}L^{3-}$, 4GDA
X

A look at structure X shows that it would be unreasonable to expect the dissociation of the third amidic group because the resulting high-energy structure would not only gain more charge but would also involve the breaking of three chelate rings (the IDA moiety) at the expense of the formation of one ring. This latter consideration results from the constraint that the ionized amide grouping must be planar.

Co(II)-*N*GDA. Co(II)-2GDA. At $a = 0$, there are actually

several species present in the solution. Because of the relatively low formation constant, there are in solution two free-ligand forms H_2L^- and H_3L and two chelate forms CoHL and CoL^-. The spectrum of CoHL was therefore picked out from a comparison of spectra measured at intermediate a values between $a = 0$ and $a = 3$. It was found that CoHL possesses an absorption at 1727 cm^{-1} for the terminal carboxylate bearing a proton. The amide group is clearly bound to the metal ion in that it shows an absorption at 1645 cm^{-1}, and the remaining band at 1625 cm^{-1} is associated with the coordinated diacetic acid carboxylates, as shown in II (with a proton on the C-terminal carboxylate).

At $a = 3$, the terminal carboxylate is completely deprotonated and now absorbs at 1603 cm^{-1}. The amide absorption at 1647 cm^{-1} indicates that it is still bound to the Co(II) ion. The bound diacetic acid carboxylates now absorb lower at 1615 cm^{-1}, a fact which could be indicative of the influence of the neighboring dissociated terminal carboxylate.

At $a = 4$, the peptide group dissociates with the metal binding now to the nitrogen. This drops the absorption frequency of the amide stretching mode down to 1580 cm^{-1}, consistent with XI containing an adjacent, bound, ionized carboxylate.

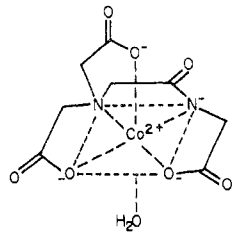

$CoH_{-1}L^{2-}$, 2GDA
XI

As a consequence of this rearrangement, the terminal carboxylate is now in a position to bind with the metal ion and therefore appears at *ca.* 1594 cm^{-1} lowered by the presence of an adjacent ionized amide group. If it were not bound to Co^{2+}, it would have absorbed at a much lower frequency, possibly 1560 cm^{-1} (because of the neighboring ionized amide). The diacetic acid moiety bound to the metal ion is represented by the vibration at 1620 cm^{-1}.

Co(II)-3GDA. The absorption spectrum for CoHL was similarly determined as in the case of 2GDA-Co. The band at 1643 cm^{-1} clearly indicates that Co^{2+} is coordinated to an amide oxygen and the other amide absorbs at *ca.* 1665 cm^{-1}. The carboxylates bound to the metal ion are represented by the absorption at *ca.* 1620 cm^{-1}, whereas the unbound carboxylate bearing a proton has a frequency of 1728 cm^{-1} associated with its unsymmetrical vibration.

The nonprotonated chelate at $a = 3$ is CoL^-. The carboxylate absorbs in the usual (at 1600 cm^{-1}) area. The amide band positions remain virtually unchanged from those above. The acetic acid carboxylates (just like those of 2GDA) show a drop in frequency down to *ca.* 1613 cm^{-1}.

The predominant species at $a = 4$ is the amide-dissociated chelate $CoH_{-1}L^{2-}$ (XII) with the cobalt ion bound to nitrogen. This ionized amide possesses an absorption at ∿1595 cm^{-1} with its neighboring oxygen coordinated to metal peptide at *ca.* 1645 cm^{-1}. The diacetic acid carboxylates coordinated to cobalt(II) ion vibrate at *ca.* 1620 cm^{-1}. The terminal carboxylate (ionized and uncoordinated) absorbs also at ∿1595 cm^{-1}.

An additional proton is dissociated at $a = 5$ (XIII). The

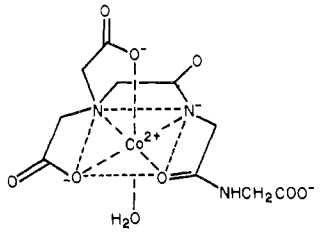

$CoH_{-1}L^{2-}$, 3GDA
XII

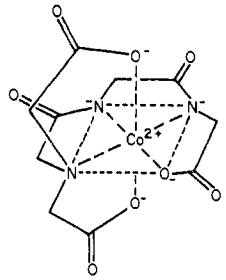

$CoH_{-2}L^{3-}$, 3GDA
XIII

adjacent isomerized and coordinated amides absorb at *ca.* 1570 cm^{-1}, the chelated IDA-type carboxylates absorb at 1618 cm^{-1}, and the ionized and coordinated terminal carboxylate shows an absorption at *ca.* 1590 cm^{-1}. This latter value would most certainly be lower were it not for coordination to the metal ion.

Co(II)-4GDA. CoHL possesses an amide O-coordinated to the metal ion (1647 cm^{-1}) and two uncoordinated amides (*ca.* 1660 cm^{-1}). The un-ionized terminal carboxylate of this chelate is at 1729 cm^{-1} and the coordinated diacetic acid carboxylates are situated at 1621 cm^{-1} in the spectrum. As base is added to $a = 3$, the species CoL^- is obtained in solution. The O-coordinated amide absorbs at 1648 cm^{-1} and the other uncoordinated ones absorb somewhat higher at *ca.* 1670 and 1663 cm^{-1}. The IDA-type carboxylates bound to a cobalt(II) ion show the usual absorbance at 1613 cm^{-1} and uncoordinated terminal ionized carboxylate shows its absorption at 1602 cm^{-1}.

At $a = 4$ (XIV), one amide group is dissociated with the

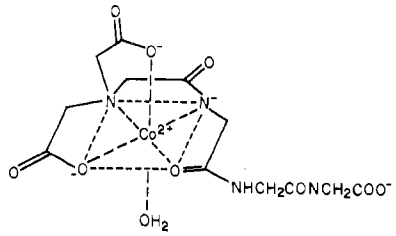

$CoH_{-1}L^{2-}$, 4GDA
XIV

usual rearrangement to M-N bonding lowering the absorption frequency of this peptide group to 1599 cm^{-1}. Now the middle amide is coordinated through its oxygen atom and is characterized by the absorption at *ca.* 1645 cm^{-1}. The uncoordinated amide absorbs at *ca.* 1670 cm^{-1}. The position of the diacetic acid carboxylates which are bound to the Co^{2+} ion is not much changed at 1615 cm^{-1}. The ionized, uncoordinated terminal carboxylate under the influence of the rest of the molecule absorbs now also at ∿1599 cm^{-1}.

When the second amido group is ionized with the addition

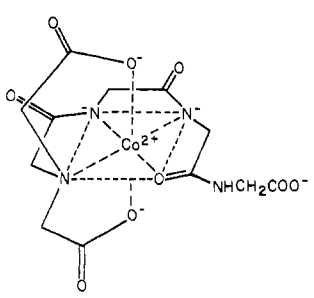

$CoH_{-2}L^{3-}$, 4GDA
XV

of more base ($a = 5$), the 1670-cm^{-1} band disappears and two types of amidic carbonyls can be distinguished from the spectrum. The two N-coordinated negative amides absorb at 1570 cm^{-1} and the O-coordinated neutral amide absorbs at 1645 cm^{-1}. The IDA-coordinated carboxylates are at *ca.* 1613 cm^{-1} and the ionized terminal carboxylate absorbs at 1596 cm^{-1}. This structure is best represented by XV.

Conclusions

Once again it was found that the derivatization of the amino group is a tool of immense importance for the study of metal ion interactions with specific donor groups.

Specifically, the addition of two acetic acid groups onto the amino groups at diglycine, triglycine, and tetraglycine achieved the following results.

1. The metal:ligand interaction stoichiometry was fixed at exactly 1:1, thus greatly simplifying the interpretation of the data. In contrast, the parent oligopeptides bind with Ni(II) and Cu(II) also in ratios of 1:2 and 1:3.
2. The mechanism of metal ion incorporation into the ligand was fixed from the amino nitrogen end of the molecule. The polyglycines react with either end depending on the metal ion.
3. The study of peptide interaction with Co(II) (and Fe(III) with some success[2a]) was made possible. Previously, metal ions such as Co(II) precipitated before the pH could be raised high enough to observe the desired interaction with the groups under study.
4. Perhaps most important of all was the new, unequivocal assignment of the band at *ca.* 1560 cm^{-1} as arising from the group frequency belonging to two adjacent N-coordinated (negatively charged) peptide groups.

Throughout the infrared study, a further conclusion became more strongly evident. Coordinated carboxylates mitigate the ability of the metal ion to polarize peptide linkages. Thus for example, Ni(II) which is hexacoordinate (possessing one more bound acetate than tetracoordinate Cu(II)) will always assist in the ionization of amide groups at a higher pH than Cu(II) will. Or, comparing *N*G with *N*GDA, all chelate amide proton association constants are higher for a given metal ion in the case of *N*GDA as compared to *N*G.

Registry No. $BrCH_2CO_2H$, 79-08-3; $H_2NCH_2CONHCH_2CO_2H$, 556-50-3; $H_2NCH_2CONHCH_2CONHCH_2CO_2H$, 556-33-2; $H_2NCH_2CONHCH_2CONHCH_2CONHCH_2CO_2H$, 637-84-3; H_32GDA, 43101-36-6; H_33GDA, 43068-75-3; H_34GDA, 43101-37-7; CuH2GDA, 43116-09-2; Cu2GDA$^-$, 43116-10-5; $CuH_{-1}2GDA^{2-}$, 43116-11-6; NiH2GDA, 43116-12-7; Ni2GDA$^-$, 43116-13-8; CoH2GDA, 43116-14-9; Co2GDA$^-$, 43064-73-9; $CoH_{-1}2GDA^{2-}$, 43116-15-0; ZnH2GDA, 49567-93-3; Zn2GDA$^-$, 43116-16-1; FeH2GDA$^+$, 43116-17-2; Fe2GDA, 43116-18-3; CuH3GDA, 43116-19-4; Cu3GDA$^-$, 43116-20-7; $CuH_{-1}3GDA^{2-}$, 43116-21-8; $CuH_{-2}3GDA^{3-}$, 43116-22-9; NiH3GDA, 43116-23-0; Ni3GDA$^-$, 43116-24-1; $NiH_{-1}3GDA^{2-}$, 43116-25-2; CoH3GDA, 43116-26-3; Co3GDA$^-$, 43116-27-4; $CoH_{-1}3GDA^{2-}$, 43116-28-5; $CoH_{-2}3GDA^{3-}$, 43116-29-6; ZnH3GDA, 43116-30-9; Zn3GDA$^-$, 43116-31-0; FeH3GDA$^+$, 43117-67-5; Fe3GDA, 43117-68-6; CuH4GDA, 43117-69-7; Cu4GDA$^-$, 43117-70-0; $CuH_{-1}4GDA^{2-}$, 43117-71-1; $CuH_{-2}4GDA^{3-}$, 43117-72-2; NiH4GDA, 43117-73-3; Ni4GDA$^-$, 43117-74-4; $NiH_{-1}4GDA^{2-}$, 43117-75-5; $NiH_{-2}4GDA^{3-}$, 43117-76-6; CoH4GDA, 43117-77-7; Co4GDA$^-$, 43117-78-8; $CoH_{-1}4GDA^{2-}$, 43117-79-9; $CoH_{-2}4GDA^{3-}$, 43117-80-2; ZnH4GDA, 43117-81-3; Zn4GDA$^-$, 43117-82-4; FeH4GDA$^+$, 43117-83-5; Fe4GDA, 43117-84-6.

Contribution from the Department of Chemistry, Case Western Reserve University, Cleveland, Ohio 44106

Copper(II) Chelation Kinetics. III. Steric Effects

J. W. BRUBAKER, Jr., A. F. PEARLMUTTER, J. E. STUEHR,*[1a] and T. V. VU[1b]

Received April 16, 1973

Rate constants for the formation of Cu(II) complexes with valine and bicine (*N,N*-dihydroxyethylglycine) have been measured by stopped-flow and temperature-jump spectrometry. The forward rate constants for valine were 1.1×10^9 and 2.3×10^8 M^{-1} sec^{-1} for mono and bis complex formation, respectively; for bicine, the corresponding rate constants were 9.5×10^8 and 3.2×10^7 M^{-1} sec^{-1}. When compared with rate constants for less hindered amino acids, these results show that steric effects are more pronounced for bis complex formation, particularly when bulky groups are coordinated to the amino nitrogen.

Of the transition metal ions Cu(II) is one of the most kinetically labile.[2] As a result, kinetic investigations involving this metal ion have been particularly difficult. However, if the protonated form of a ligand is relatively unreactive, Cu(II) complexation reactions involving the free ligand may be studied at low pH values where the concentration of reactive ligand is greatly reduced.[3] By means of this technique, a series of copper(II)-amino acid reactions have been characterized.[3-8] From these investigations the following generalizations can be made. (1) The rate constant for the formation of the mono complex from the anionic form of the amino acid is on the order of $(1\text{-}3) \times 10^9$ M^{-1} sec^{-1}. (2) In all instances the major kinetic pathway involves reaction with the unprotonated ligand, with only small or negligible contributions from the zwitterionic form. (3) The rate constant for the formation of the bis complex is never larger than that for the mono and, in many instances, has been found to be much smaller.[3-8] (4) The formation rate constants for β-amino acids (six-membered chelate rings) are smaller than

(1) (a) NIH Career Development Awardee. (b) NSF Summer Undergraduate Research Participant.

(2) M. Eigen, *Pure Appl. Chem.*, 6, 97 (1963).

(3) (a) A. F. Pearlmutter and J. Stuehr, *J. Amer. Chem. Soc.*, 90, 858 (1968); (b) W. B. Makinen, A. F. Pearlmutter, and J. Stuehr, *ibid.*, 91, 4083 (1969).

(4) R. L. Karpel, K. Kustin, and R. F. Pasternack, *Biochim. Biophys. Acta*, 177, 434 (1969).

(5) R. F. Pasternack, E. Gibbs, and J. C. Cassatt, *J. Phys. Chem.*, 73, 3814 (1969).

(6) R. L. Karpel, K. Kustin, A. Kowalak, and R. F. Pasternack, *J. Amer. Chem. Soc.*, 93, 1085 (1971).

(7) R. F. Pasternack, K. Kustin, L. A. Hughes, and E. Gibbs, *J. Amer. Chem. Soc.*, 91, 4401 (1969).

(8) V. S. Sharma and D. L. Leussing, *Inorg. Chem.*, 11, 138 (1972).